INTERNATIONAL ATOMIC ENERGY AGENCY
UNITED NATIONS EDUCATIONAL, SCIENTIFIC AND CULTURAL ORGANIZATION

INTERNATIONAL CENTRE FOR THEORETICAL PHYSICS
34100 TRIESTE (ITALY) - P.O.B. 586 - MIRAMARE - STRADA COSTIERA 11 - TELEPHONE: 2240-1
CABLE: CENTRATOM - TELEX 460392 - I

H4.SMR 346/19

SCHOOL ON
NON-ACCELERATOR PHYSICS
25 April - 6 May 1988

OPTICAL AND X-RAY OBSERVATIONS OF THE SUPERNOVA 1987A

by

J. Danziger
E. S. O.
Munchen
F. R. Germany

SN.

John Danziger
E.S.O.
30 April 1988

2 TYPES BASED ON SPECTRA
(MINKOWSKI 1941)

TYPE I - NO BALMER LINES
TYPE II - PRONOUNCED BALMER LINES IN EMISSION.

MANY OTHER FEATURES COMMON TO BOTH

CLASSIFICATION BY LIGHT CURVES CAN BE MISLEADING.
CLASSIFICATION FROM IUE UV ALSO MISLEADING
THERE ARE DIFFERENCES AMONG BOTH TYPES.

CURRENTLY THERE SEEMS GOOD EVIDENCE FOR TYPE I a (1972 e) AND TYPE I b. (1983 n).

OCCURRENCE

TYPE I OCCUR IN GALAXIES OF ALL TYPES

TYPE II OCCUR ONLY IN SPIRAL GALAXIES AND HAVE STRONG ASSOCIATION WITH SPIRAL ARMS.

UNTIL SN 1987 a NO TYPE II HAD BEEN RECORDED IN MAGELLANIC TYPE IRREGULAR GALAXIES.

...on. the observed radio emission originates ... Within this frame, it is clear that a strong ... the involved binary system is relatively ... event.

... are not a totally uncommon occurrence ...3 (Bertola, 1964) and SN 1964l in NGC ... similar to those of SN 1983n. the 6150 Å ...ther slow and the magnitude at maximum ...ering the frequency of Type I SNe as a ... Fig. 9) one finds that, while in elliptical ...nd $M_B \sim -20^m$ with a small dispersion, ...ain peak around $M_B \sim -20^m$ but extends ...entered around $M_B \sim -18^m$ and contains ...Type I SNe in spiral galaxies. Moreover, ...redder colours than average, just the same ...e fainter magnitude of these SNe could ... colours. However, the level of extinction ...agnitudes is unreasonably high for such a ...t in the case of SN 1983n the extinction ... Therefore, it is more likely that spiral ... exist in early type galaxies. They would ...assive binary systems in which neither of ...e II SN.

Type I SNe in late type galaxies unsuited ... measurements should be made to clarify ... However, it is not even clear yet whether ... two sharply separated groups or rather ...emely anomolous subtypes, which would ...defined.

...s clear that Type II SNe can be used for ... method. To derive meaningful distances ... of the event, say from maximum light

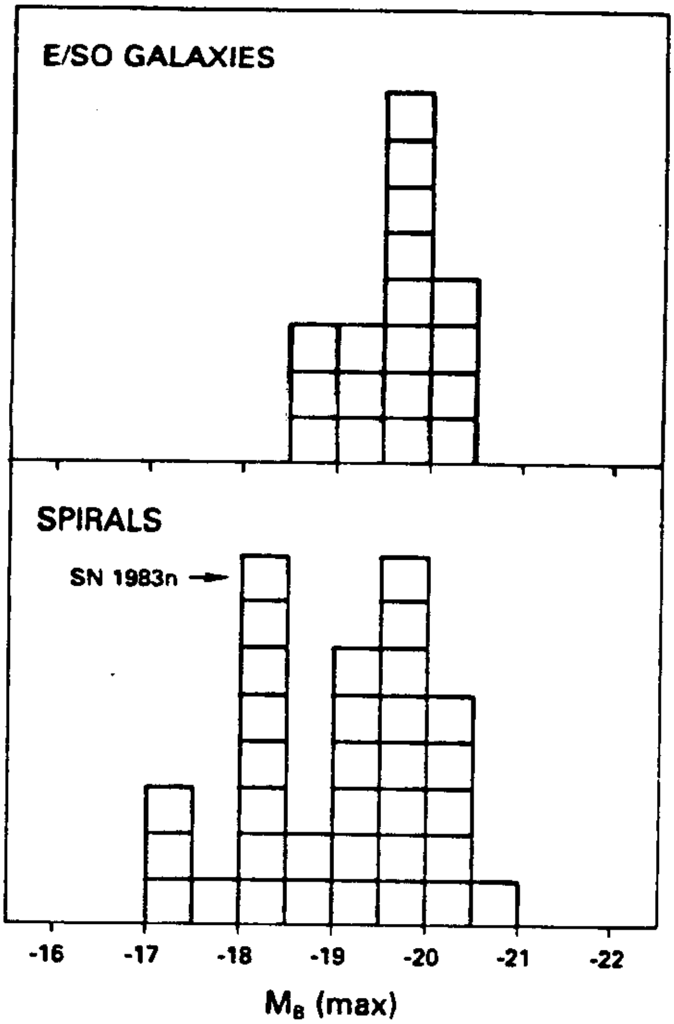

Figure 9. The distribution of Type I SNe as a function of the absolute B magnitude for E/S0 galaxies (upper panel) and for spiral galaxies (lower panel). The box containing SN 1983n is explicitely marked.

CURRENT SN RATES (VAN DEN BERGH, McCLURE, EVANS)

I a	I b	II
$0.3\ h^2$	$0.4\ h^2$	$1.1\ h^2$

PER 10^{10} $L_B(\odot)$ PER 100 YEARS

∴ 2 PER CENTURY IN GALAXY

≥ 0.16 " " " LMC.

GENERAL CHARACTERISTICS TYPE I

PHASE A : 0 - 20 DAYS AFTER MAXIMUM.

SMOOTH CONTINUUM SUPERPOSITION OF P CYGNI PROFILES

EMISSION PEAKS : 3950, 4600, 5180, 5900 8600 Å.

STRONG ABSORPTION AT 6150 Å.

WEAKER FEATURES STRENGTHEN WITH TIME

PHASE B : 60 - 100 DAYS
CONTINUUM REDDER

EMISSION PEAKS AS ABOVE. ANOTHER COMPLEX FEATURE AT 4900 Å.

BROAD FEATURE 5180 - 5600 WITH EMISSION PEAK AT 5600.

EMISSION BAND AT 6550 (Hα ?)

PHASE C : ~~60~~ 100 - 200 DAYS SUBTLE CHANGES

5600 Å FEATURE DISAPPEARS

PHASE D. : 200 - 400 DAYS.

STRONG CHANGES

ABSORPTION SHORTWARD OF EMISSION PEAKS NEAR 3950, 5910, 8600 Å.

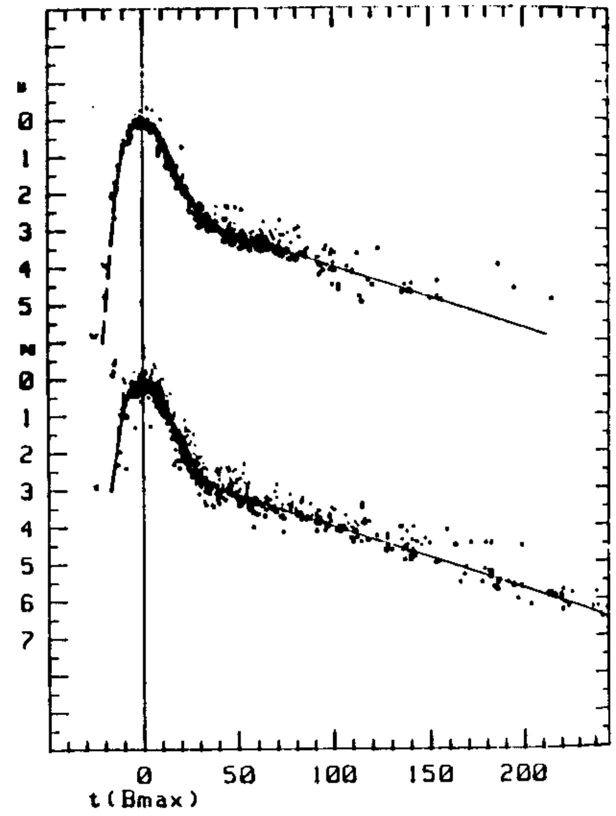

Fig. 1. The composite pg light curve for 16 SNeI (lower curve) and the composite B light curve for 22 SNeI. The adopted templet light curves are shown as full lines. Note the smaller scatter in B than in pg.

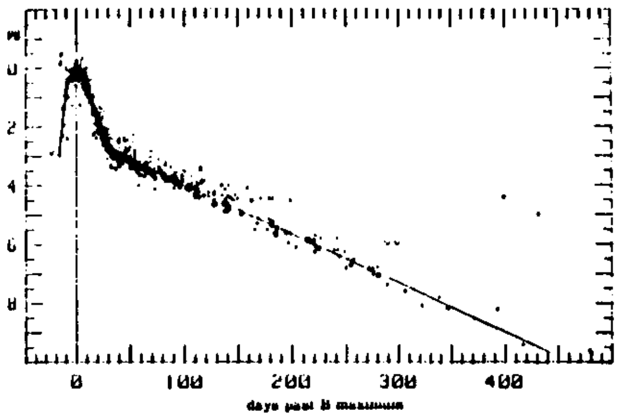

Fig. 2. The composite pg light curve of 16 SNeI. Same as Fig. 1, lower curve, but here extending to almost 500 days.

background light, which may become particularly severe for photoelectric observations. For this reason the decline rate during the exponential phase should be taken only as an approximation.

SNeI can be distinguished from SNeII unambiguously only from spectroscopy. Not for all objects in Fig. 1 and 2 spectroscopy is available. But most objects lacking spectroscopy have occurred in E galaxies and this is generally taken to be sufficient evidence for a type I assignment, because all spectroscopically investigated SNe in E galaxies have so far proven to be of type I. It is, however, possible that Fig. 1 and 2 still contain a few objects which are not genuine SNeI. This possibility can only strengthen our conclusion, that true SNeI define a templet light curve which they follow to within the observational error.

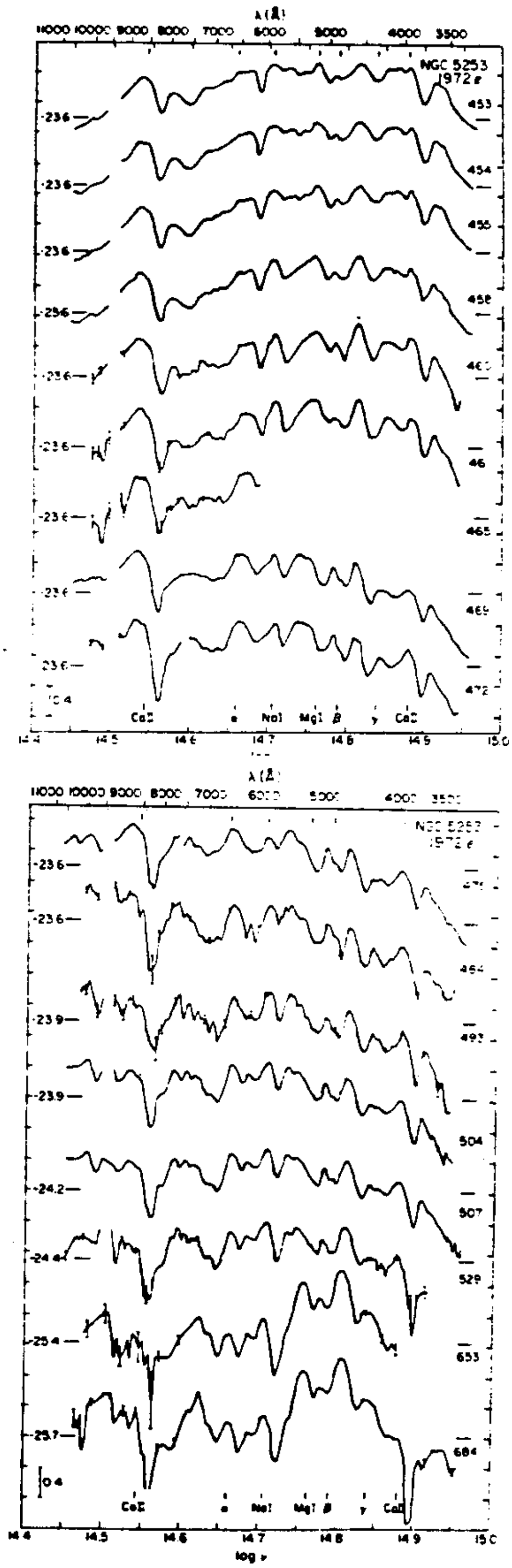

FIG. 7.—Continuation of fig. 6

EMISSION PEAKS AT 6550, 7200
5300, 4750 (DRIFTED IN TIME FROM
4600 Å).

IDENTIFICATIONS WILL BE DISCUSSED
BELOW.

TYPE I L LACK 6150 Å FEATURE.

TYPE II

GREATER DIVERSITY AMONG TYPE II
ALTHOUGH LINE IDENTIFICATION EASIER.

PHASE A : 0-20 DAYS.

FEW DAYS AFTER MAXIMUM.
SMOOTH CONTINUUM Hα MOST
CONSPICUOUS SPECTRAL FEATURE.

Hβ, Hγ HAVE P CYGNI PROFILES.
AS DO FEATURES AT 3950 Å AND
5150, 5900 Å.

ABSORPTION IN P CYGNI INCREASING.

PHASE B : 20-70 DAYS

CONTINUUM SMOOTH AND REDDER
ABSORPTION INCREASING. STRONG Hα EMISSION
STRONG P CYGNI AT 8600 Å. MOST
PROMINENT STRONG EMISSION BAND AT 4600 Å

LATE PHASE : CONTINUUM STILL PRESENT
Hα EMISSION [OI] 6300
[Ca II] 7295 EMISSION

resolution of 40 and 80 Å. The exceptions are multichannel observations made in 1972 December and 1973 January.

Observations were made in such a way that the entire spectrum was covered and no gaps occurred. Observations between 8900 and 9700 Å are somewhat uncertain because of the strong water-vapor absorption in the Earth's atmosphere. In particularly bad cases the observations were completely deleted over this wavelength range. This water-vapor absorption problem was particularly serious in SN 1972e which, because of its southerly declination, was always observed at large zenith distances. In some cases a nearby comparison A-type star, Boss 18446, was observed at the same time and with the same bandpasses as the supernova. It was then possible to correct accurately for the water-vapor extinction. In a few cases the extinction in the atmospheric *A*-band was not properly determined, and those observations have been deleted. The spectral energy distributions are based on the absolute calibration of α Lyrae given by Oke and Schild (1970).

Absolute spectral-energy distributions are plotted in figures 1–7 where $\log f_\nu$, the logarithm of the spectral flux density (ergs s^{-1} cm^{-2} Hz^{-1}) is plotted against $\log \nu$,

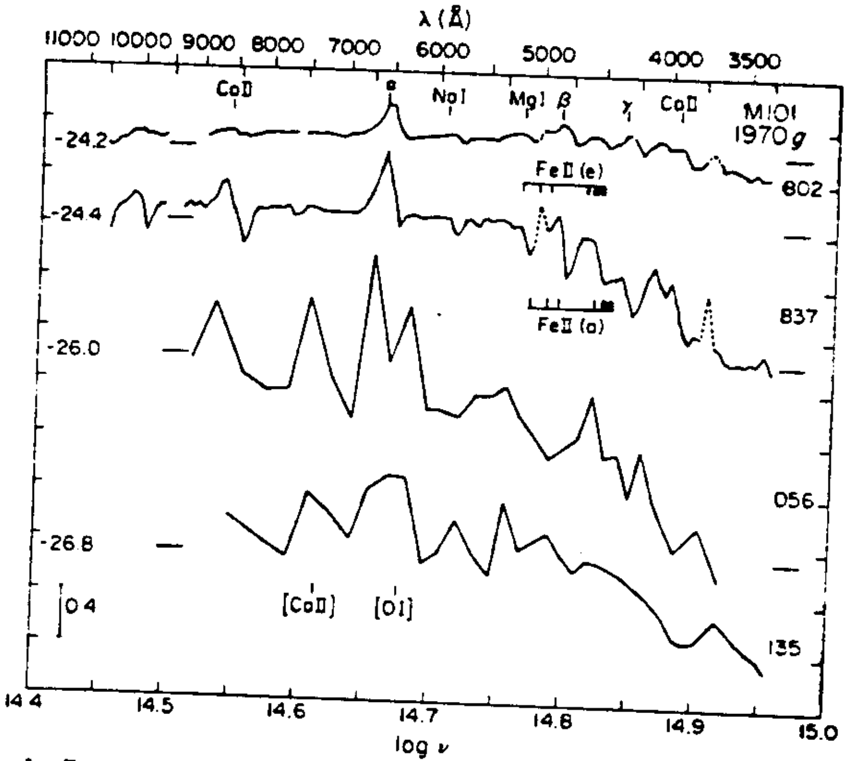

FIG. 3.—Energy distributions for the Type II SN 1970g in NGC 5457 (M101). Description is the same as fig. 1. Dotted portions of the top two energy distributions are the emission lines λ3727 of [O II] and λ5007 of [O III] which are emitted by the H II region on which the supernova is projected. For the bottom two energy distributions the background H II region (which had been previously observed [Searle 1971]) has been subtracted as well as possible. Possible line identifications of the emission peaks are marked. Positions of the strongest expected Fe II lines are shown. Emission wavelengths are plotted without velocity corrections. Absorption wavelengths are displaced by 0.008 in log ν to the violet, corresponding to the best fit of the absorption minima.

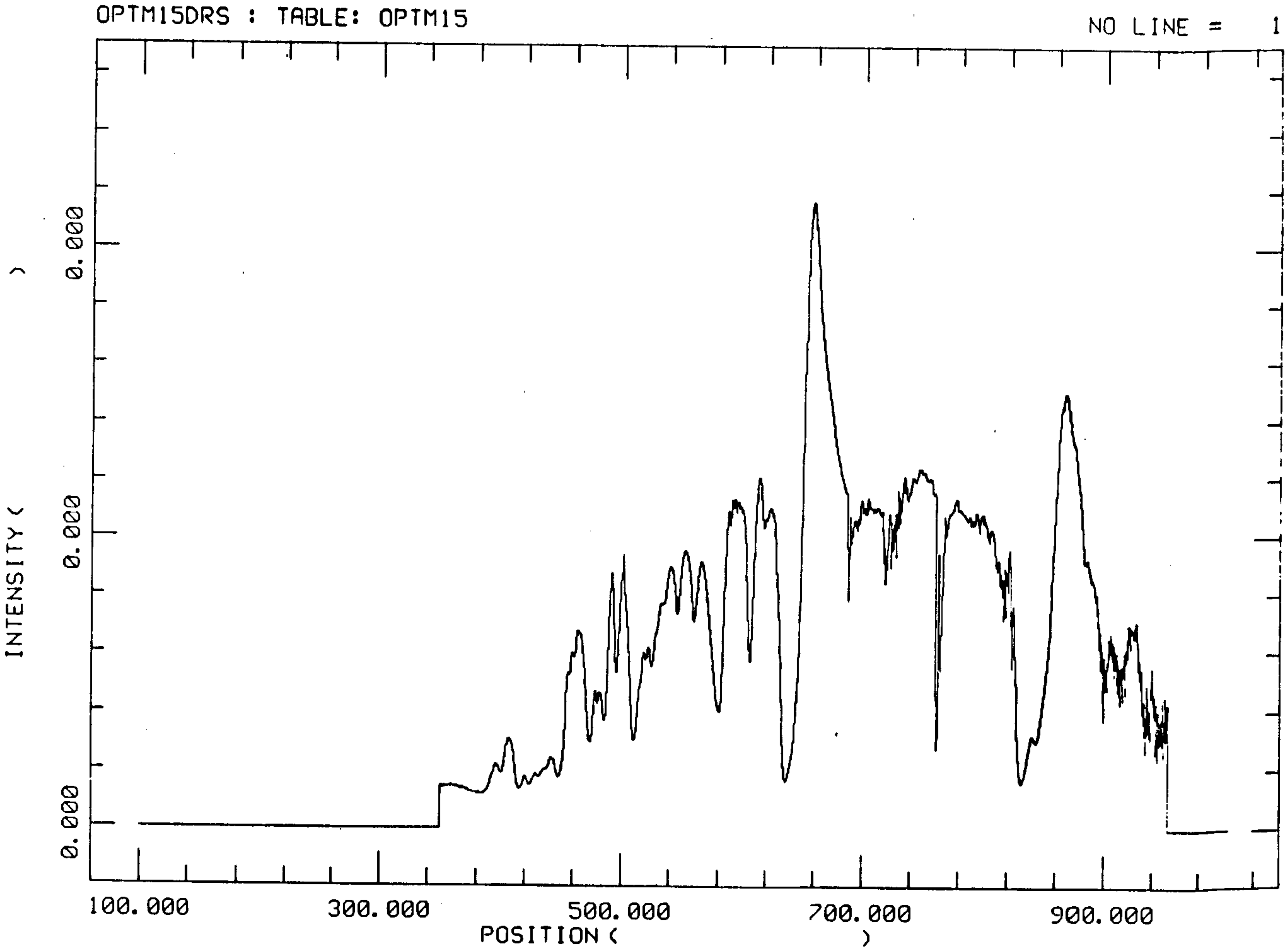

OPTM15DRS : TABLE: OPTM15
NO LINE = 1
0.000
0.000
0.000
INTENSITY ( )
100.000
300.000
500.000
700.000
900.000
POSITION ( )

GENERAL FEATURES

OPAQUE COOLING EXPANDING ENVELOPE THAT RESEMBLES ATMOSPHERE OF SUPERGIANT

TEMPERATURE RANGE

10 000 K END OF MAXIMUM
5000 K AFTER 20 DAYS.
PRE-MAXIMUM DATA SUGGESTS TEMPERATURES
>> 10 000 °K
P-CYGNI PROFILES SUGGEST RESONANCE SCATTERING IN EXPANDING ENVELOPE.

VELOCITIES	I	II
ABSORPTION MINIMUM	12 000 KM/SEC	7000
VIOLET EDGE OF ABSORPTION	20,000	15000

SN 1987 a ATYPICAL.

LINE IDENTIFICATIONS

TYPE I

Ca II H & K (3950), Mg I (5180), Na D (5890)
Ca II IR (8600). Hα 6550.

TYPE II

\+ OTHERS Fe I, Fe II, Ti II, Sc II. Si II 6100

BALMER LINES, Ca II H & K (3950) He I 5876
Ca II IR TRIPLET (8600) Na I D
Mg I b Fe II Mg II 4481
[O I] 6300, [Ca II] 7295, 7323.

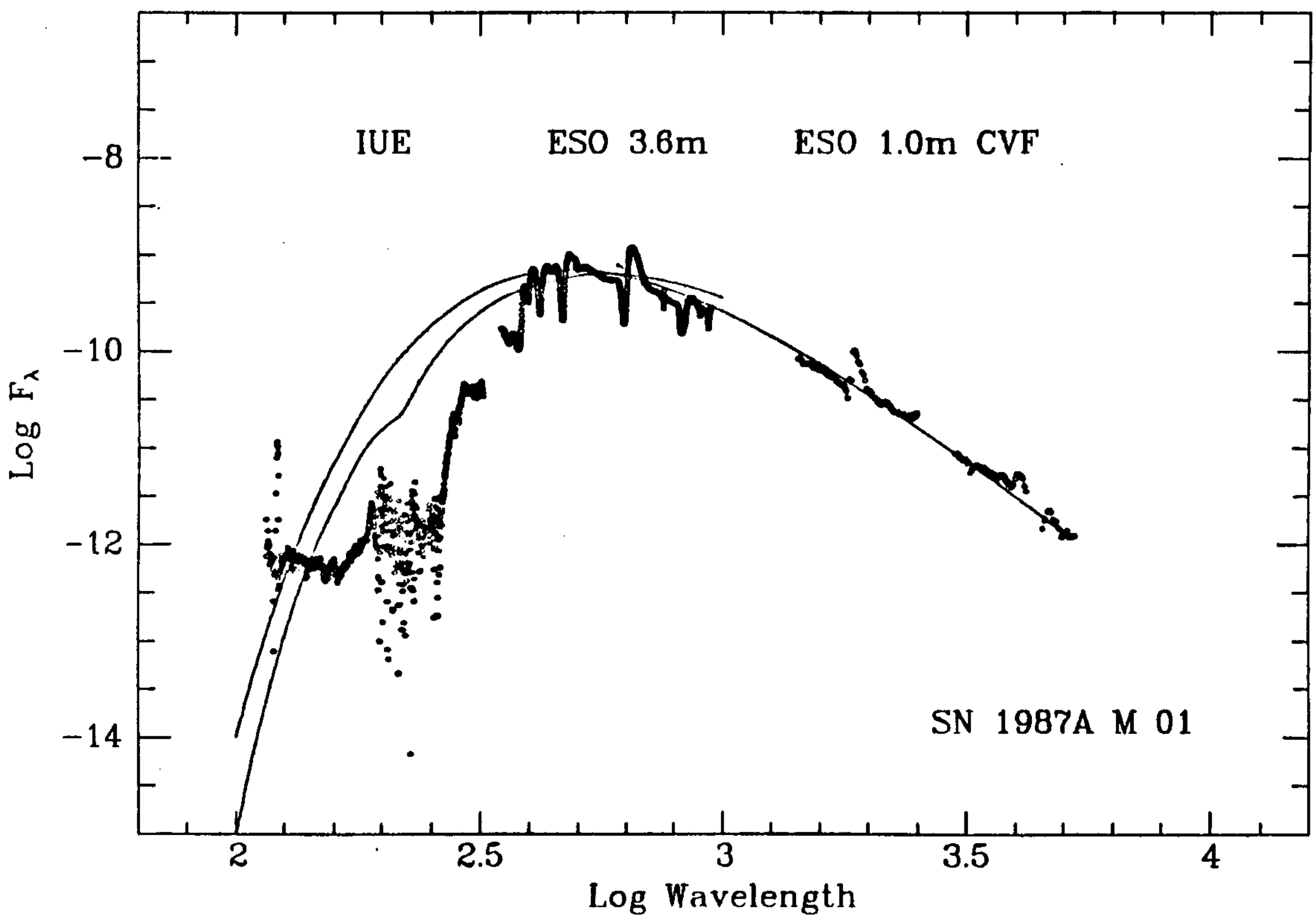
IUE
ESO 3.6m
ESO 1.0m CVF
SN 1987A M 01
Log F_λ
Log Wavelength
-8
-10
-12
-14
2
2.5
3
3.5
4

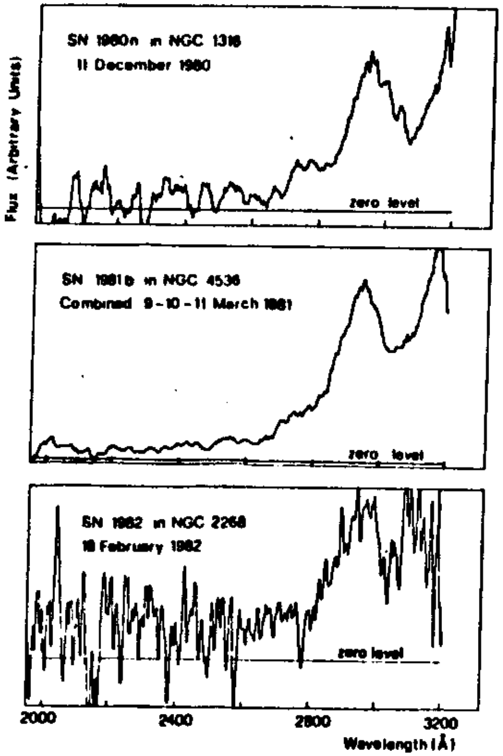

Figure 4. The IUE long wavelength spectra of Type I Supernovae. Note the prominent emission feature centered at ~ 2950 Å.

So far, four Type I Supernovae have been extensively observed in the near IR, i.e. 1972e in NGC 5253, (Kirshner *et al.* 1973); 1980n in NGC 1316, 1981b in NGC 4536 and 1981a in NGC 1316 (cf. Elias *et al.* 1981 and references therein). Two of them, 1980n and 1981b, are in the IUE sample. Again a very close similarity is found in the spectral behaviour and the light variation among the observed SNe. This extends their characteristics of "standard candles" also to the infrared. Another interesting fact is that the light curves in the J, H and K bands display a first minimum 15-20 days after optical maximum, reach a secondary maximum ~ 30 days after maximum and then decay steadily at a rate of ~ 0.04 magnitudes/day. This decay rate is faster than what is observed at optical wavelengths on a long time scale.

Combining different observations, one can reconstruct the complete spectrum of a Type I SN from UV to the IR. As an illustration, the spectrum of SN 1981b at an epoch around the optical maximum is shown in Fig. 5. We see that the ultraviolet spectrum declines very steeply with the wavelength. Moreover, the ultraviolet emission is much lower than a black body extrapolation of the optical spectrum. This is just the opposite of what is found for Type II SNe (cf. Section 2.2). In particular, the UV flux is approximately 10 times lower than the black body curve at the colour temperature appropriate to match the visual spectrum ($T \approx 15000$ K, upper curve). Also, in the infrared the observed spectrum is much weaker than a black-body extrapolation from the optical. On the other hand, the IR and UV spectra can smoothly be connected to each other by a lower temperature black-body ($T \sim 9400$ K, lower curve). These results indicate that the opacity in both UV and IR must be much higher than at optical wavelengths, so that the radiation temperature is close to the effective temperature in the visual but reduces to the minimum temperature $T_{min} \sim 0.6\, T_{eff}$ both at shorter and at longer wavelengths.

Within this sample of Type I SNe only SN 1981b has been observed in the radio. It has been monitored at 5 GHz with the VLA at regular time intervals within the period March 1981–February 1983 but it has never been detected (Weiler *et al.* 1984), the upper limit to the radio flux being as low as 50 μJy (1 σ). From a comparison with the radio properties of Type II SNe, Panagia (1984a) argues that the lack of radio emission from SN 1981b implies that its progenitor was a star which in the late phase of its evolution underwent a low mass loss ($\dot{M} < 10^{-7}$ $M_\odot$ yr^{-1}) and, therefore, was a relatively low mass star (< 3 $M_\odot$).

2.4. Supernova 1983n in NGC 5236: An Anomalous Type I

On July 3rd, 1983 a bright supernova ($m_v \sim 13$ at discovery) was discovered in the southern spiral galaxy NGC 5236 = M83. The IUE observations were started on July 4th, i.e. one day after discovery, and continued at regular intervals until mid-August when the SN became too faint to be detected. The first long wavelength IUE spectrum obtained on July 4th was remarkably similar to that displayed by SN 1981b on 9-11 March, 1981, i.e. at the epoch of its maximum in the B band

MAIN OBSERVED FACTS.

1. CONTINUUM CARRIES MOST OF FLUX
2. STEADY DECREASE OF COLOUR TEMPERATURE
3. P CYGNI PROFILES.
4. DIFFERENT EXPANSION VELOCITIES COMIN FROM DIFFERENT LINES. (ALSO IN SN 1987

OTHER FEATURES OF TYPE II

SOME WEEKS AFTER MAXIMUM

T_e (PHOTOSPHERE) ~ 5000°K

N_e (REVERSING LAYER) ~ 10^9 el cm^{-3}

2×10^{24} el cm^{-2} IN COLUMN THROUGH REVERSING LAYER → 0.3 $M_\odot$.

ELECTRON SCATTERING MAIN OPACITY.

CHEMICAL ABUNDANCES — SOLAR

DEFICIENCY OF UV FLUX WHEN FITS OF BLACK BODY CURVES MADE TO IR + V SPECTRUM.

APPEARANCE OF OI 6300 AND CaII 7300 Å AFTER 8 MONTHS SUGGESTS SIGNIFICANT QUANTITIES OF HOT GAS WITH $N_e < 10^5$ cm^{-3}.

Ca II

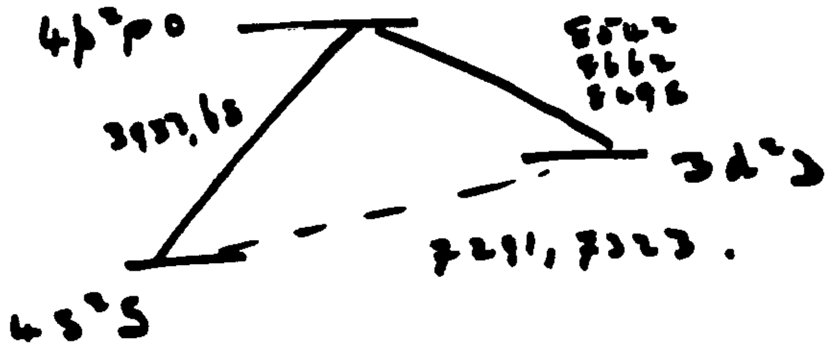

WHEN DENSITY HIGH ONLY ALLOWED TRANSITIONS SEEN. AT LOW DENSITY FORBIDDEN TRANSITIONS ARE IMPORTANT.

1979 C IN M 100. PANAGIA ET. AL (1980) BRANCH ET. AL (1981)

NO P CYGNI IN Hα

COLLISIONAL EXCITATION OF Hα, Mg II 2800

MASS OF EJECTED MATERIAL ≳ 5 M$_\odot$

1983 K IN NGC 4699. NIEMALA ET AL. (1985)

PREMAXIMUM HE II 4686
N III 4640 BLEND
PRESENT.

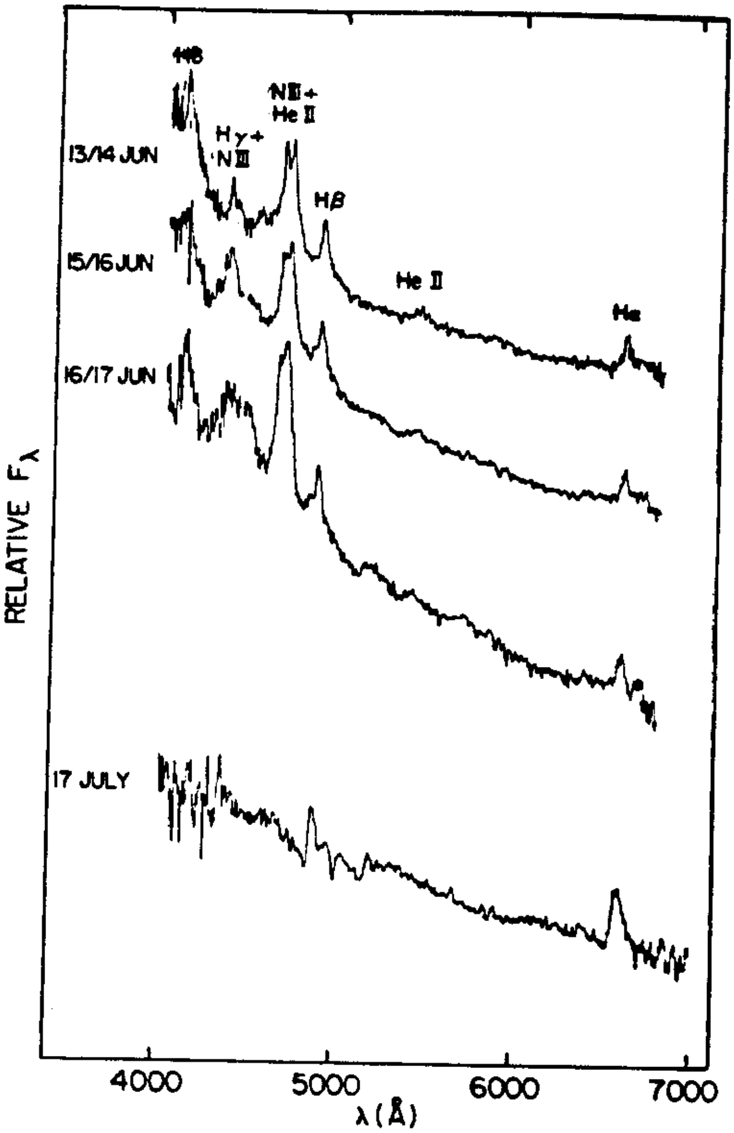

FIG. 2.—SIT Vidicon spectra of SN 1983k obtained with the CTIO 1.5 m telescope in 1983 June and July. The July spectrum is the average of observations made on 16 and 18 July (UT).

It seems likely that the H I absorption lines observed at this phase are related to the weak blueshifted absorptions seen in the first 1 m spectrum when the Wolf-Rayet-like emission lines were still present. This is supported by the radial velocity measurements, which show a steadily increasing blueshift of these features over the 11 day period from premaximum to maximum covered by the 1 m spectra. The mean of the Hγ and Hδ measurements are plotted as a function of time relative to the nuclear velocity of NGC 4699 (and corrected for the assumed contribution of galactic rotation) in Figure 4, and indicate an approximately linear acceleration rate of 40 km s^{-1} day^{-1}. The velocities for this absorption are quite low and the line profiles much narrower in comparison with the absorption lines observed in the postmaximum spectra of August 1 and 2 (see below), and those seen in other Type II supernovae at comparably late epochs (e.g., see Kirshner and Kwan 1974).

gue table I

Plate No.	Date	UT	Exposure (minutes)	m_{pg}
2276	10	23 24	10	12.70
2279	11	17 13	10	12.50
2292	12	17 46	10	12.85
2294	14	22 53	10	12.71
2305	15	23 59	10	12.90
2313	17	26 12	10	13.46
2323	25	17 05	10	14.04
2329	27	21 03	10	14.20
2330	Jan. 1, 1962	20 07	10	14.54
2332	4	20 09	10	15.10
2364	6	17 22	10	15.25
2403	8	17 44	10	15.20
2422	12	24 07	10	15.35
2440	23	17 30	10	15.60
2448	24	18 41	10	15.35
2454	25	17 38	10	15.60
2470	27	17 46	10	15.70
2471	27	18 25	10	15.75
2496	29	18 01	10	15.70
2524	31	18 47	10	15.50
2544	Feb. 2	17 38	10	15.40
2578	4	20 02	10	16.00
2601	6	17 59	10	15.90
2624	20	18 07	7	15.80
2630	23	18 40	10	16.30
2653	Mar. 7	18 45	10	16.70
2675	28	18 55	13	16.70
2696	April 2	19 07	10	)16.00
2706	5	20 15	10	)16.00
2718	7	19 30	7	)16.00
2964	July 9	25 35	10	16.70
2971	10	25 27	10	)16.00
5151*	26	25 30	40	16.70
5159*	27	25 47	45	16.69
5175*	Aug. 1	25 57	20	16.68
5185*	8	25 51	45	16.70
5227*	26	24 30	30	16.70
5243*	30	26 20	30	16.80
5254*	Sept. 2	25 25	15	16.72
5070	8	24 42	8	16.70
5274*	8	25 40	40	16.74

ne star is sufficiently far from the center of the galaxy so as not to be bedded in nebulosity. In fig. 3 the light curve of the variable is plotted ing the data of Table I. This curve has a very unusual appearance n h is very difficult to reconcile with that of other known types of riables and may be briefly described in the following manner:

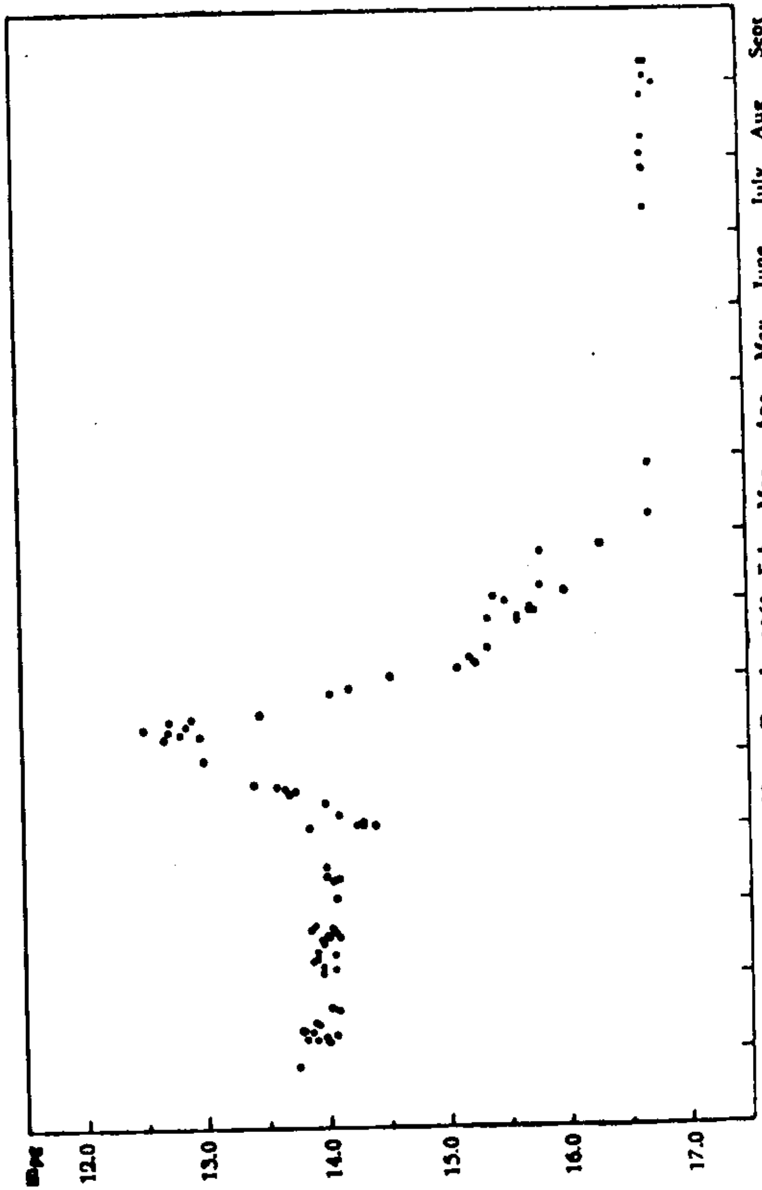

Fig. 3. — The light curve of the variable near NGC 1058. The dots and circles refer to the Schmidt and 122 cm reflector observations respectively

TYPE I

KIRSHNER ET AL. (1975)
MEYEROTT (1980)

1972 e IN NGC 5253

OVERABUNDANCE OF FE (20× COSMIC) SUGGESTED TO EXPLAIN OBSERVED FEATURES IN RANGE 4200 - 5500 Å. THIS RESULTS FROM INCLUSION OF > 100 [Fe II] LINES IN THIS REGION. 4600 Å FEATURE NOT EXPLAINED. POSSIBILITY OF

Mg I 4571 INTERSYSTEM LINE ($^3P_2 \rightarrow {}^1S_0$ A~400)

COLLISIONAL EXCITATION PREDOMINATES WHEN CONTINUUM WEAK.

MEYEROTT EXPLAINS ALL ABOVE FEATURES WITH [Fe II] AND [Fe III] LINES.

4300, 4600, 4800, 5000, 5200, 7200.

FEATURES AT 4600 5000 REQUIRE [Fe III]

SEE SPECTRUM OF SN 1986 CEN A.

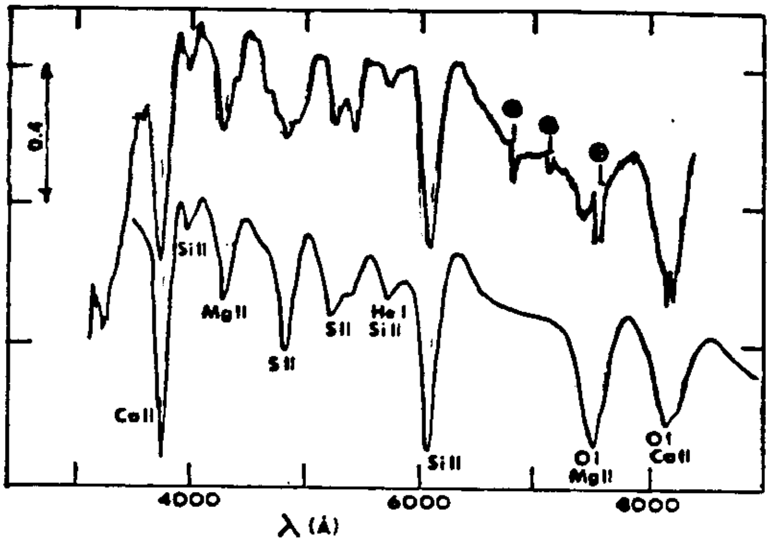

Figure 1. Upper: a McDonald Observatory spectrum of the SN I of 1981 in NGC 4536 at maximum light. Lower: A synthetic spectrum having T = 17,000 K, V = 12,000 km/sec, and A_V = 0.3.

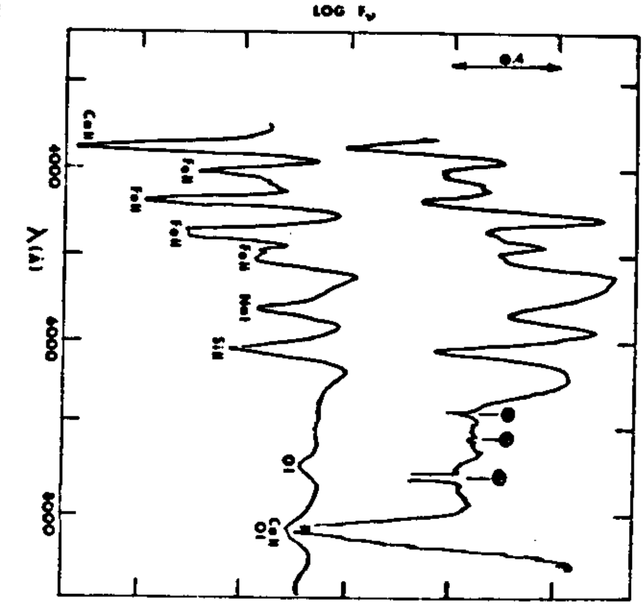

Figure 2. Upper: McDonald Observatory spectrum of the SN I of 1981 in NGC 4536, 17 days after maximum light. Lower: a synthetic spectrum having T = 8000 K, V = 11,000 km/sec, and A_V = 0.3.

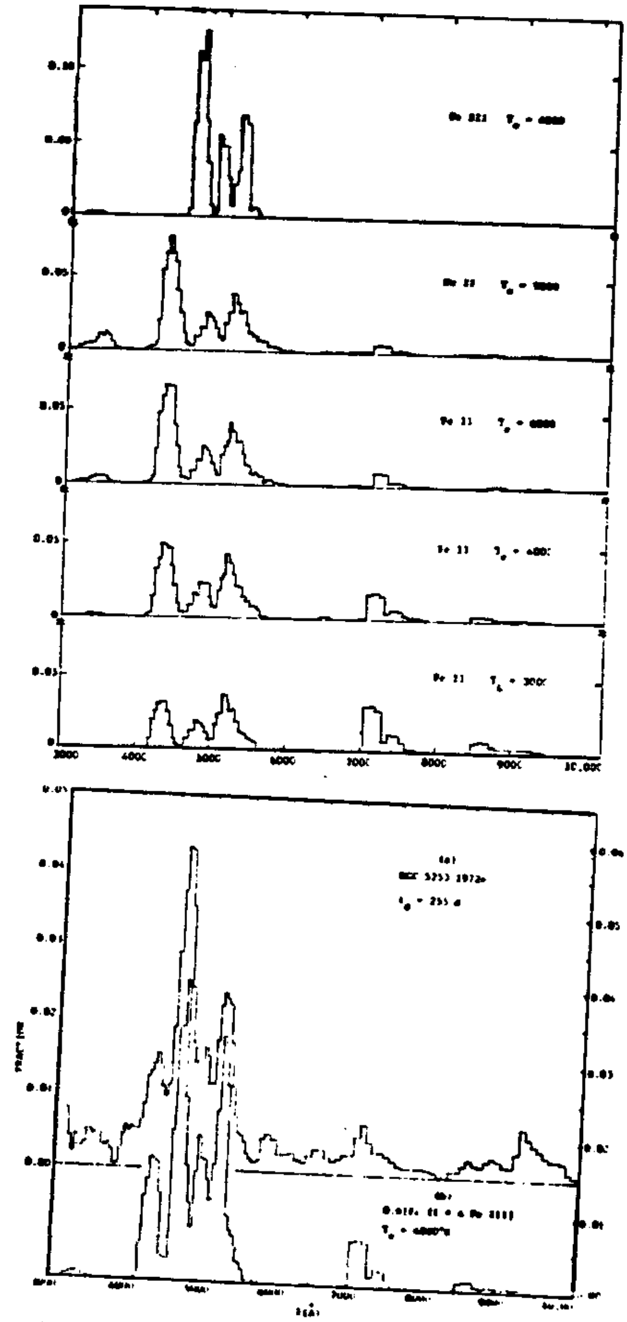

FIG. 1. (a) Ratio of the flux radiated in 40 Å to the total radiated from 3220 Å to 11,600 Å versus wavelength at t_e = 255 days. (b) Synthetic spectrum of Fe II + 4Fe III at T_e = 4000 K, normalized so that the total integral from 3220 Å to 11600 Å equals 0.6

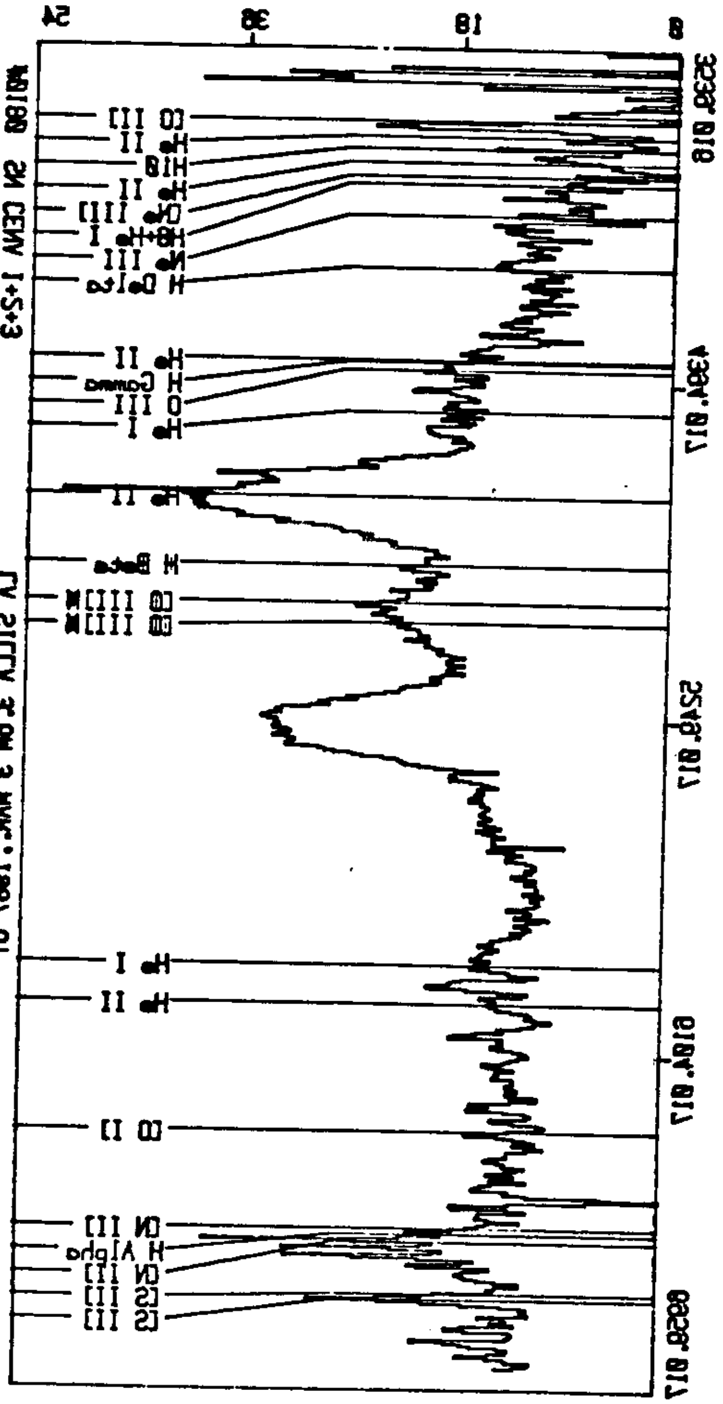
LA SILLA 3.6M 3 MAR. 1987 UT
W0180 SN CENA 1+2+3
3530.018
4394.017
5249.017
6104.017
6958.017
H Alpha
H Beta
H Gamma
H Delta

COBALT IN TYPE I ?

EVIDENCE IN TYPE Ia 1981b (BRANCH (1986))
FROM A UV SPECTRUM SYNTHESIS OF FE II
AND CO II.
SINCE 1983n IS TYPE Ib AND HAS
SIMILAR UV SPECTRUM PRE-MAX.
TO 1981b THIS SUGGESTS TYPE Ib
CANNOT COME FROM WR STARS WHICH
WOULD NOT PRODUCE CO II.

0.3 $M_\odot$ OF Fe IN TYPE Ib ??

1983n ~~MEIKLE~~ GRAHAM ET AL. (1986).

Fe II 1.644 μ OBSERVED

FEATURE MAY BE Si I.

MODEL NEEDS MODIFYING IN
VIEW OF SUBSEQUENT O-RICHNESS
OF 1983n.

EVOLUTION TO SNR

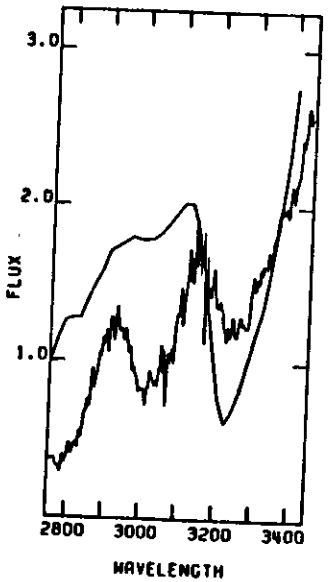

Fig 1

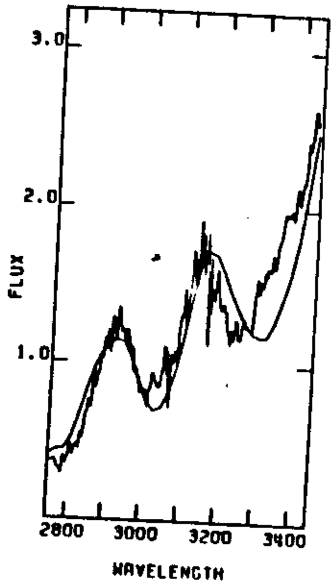

Fig 2

Fig. 1.—An observed maximum-light spectrum of SN 1981b in NGC 4536 is compared to a synthetic spectrum based on lines of Co II (smoother curve). Flux is in units of 10^{-25} ergs cm^{-2} s^{-1} Hz^{-1}.

Fig. 2.—Like Fig. 1, but the synthetic spectrum is based on lines of Fe II and Co II.

optical maximum-light synthetic spectrum: O I, Mg II, Si II, S II, and Ca II. As in the optical calculations, the line optical depths were taken to vary with radius as r^{-7}. The color temperature was taken to be 5000 K, simply to match the slope of the observed ultraviolet continuum. The velocity at the photosphere and the excitation temperature were varied. When the optical depths of the ultraviolet lines were required to be consistent with those used previously for the optical lines, the ultraviolet synthetic spectra did not resemble the observed spectrum. Even when the optical depths of the ultraviolet lines were uncoupled from those of the optical lines, and varied freely, no satisfactory fit to the observed spectrum was obtained. The spectral features in the interval 2750–3450 Å evidently are not produced by the same ions that have been invoked to explain the maximum-light optical spectrum.

In the course of the optical studies, the spectral minimum near 3250 Å had been identified tentatively as a blueshifted absorption feature produced by strong lines of singly ionized cobalt having rest wavelengths in the interval 3350–3500 Å (Branch 1985). This identification is consistent with the prevailing opinion that Type I supernova light curves are powered by the decay of ^{56}Ni through ^{56}Co to stable ^{56}Fe (Colgate and McKee 1969; Woosley and Weaver 1986, and references therein), and with the carbon-deflagration model (Branch *et al.* 1985). We therefore have computed ultraviolet synthetic spectra based solely on lines of Co II. For the synthetic spectrum shown in Figure 1, the velocity at the photosphere is 12,000 km s^{-1}, and the excitation temperature is 10,000 K, consistent with the previous optical synthetic spectra. Considering the simplicity of the resonance scattering approximation, the Co II lines do (again) provide a satisfactory explanation for the 3250 Å minimum, but they do not account for the 3000 Å minimum.

Lines of Fe II were not invoked to account for the optical maximum-light spectrum, but they did appear to dominate the spectrum beginning shortly after maximum light. An ultraviolet synthetic spectrum based on lines of both Co II and Fe II is shown in Figure 2. In this calculation, the relative strengths of the Co II and Fe II lines were fixed by assuming a Co/Fe abundance ratio of 11, as would be the case if both elements had originated from the synthesis of ^{56}Ni at the time of the explosion, about 15 days earlier. The absolute strengths of the lines were varied freely. The synthetic spectrum shown in Figure 2 provides a good match to the observed spectrum. The synthetic features are complex blends; 110 Fe II lines and 21 Co II lines have optical depths at the photosphere greater than 1. The optical depths of the ultraviolet Fe II lines correspond to an optical depth of the strongest optical Fe II line, λ5018, of about 10. This is not quantitatively consistent

SN AS DISTANCE INDICATORS

TYPE II — KIRSHNER & KWAN (1974)

TYPE I — BRANCH ET AL. (19)

MODIFICATION OF BAADE-WESSELINK METHOD

PHOTOMETRIC ANGULAR RADIUS

$$\theta = \left[f_\nu / \pi B_\nu(T) \right]^{\frac{1}{2}}$$

RADIUS OF PHOTOSPHERE

$$R = v\,(t - t_0) + R_0$$

IF t_0 NOT KNOWN OBSERVE v AT 2 EPOCHS WELL APART.

R_0 ASSUMED SMALL

$$D = \frac{v_2\,(t_2 - t_1) + R_0\left(1 - v_2/v_1\right)}{\theta_2 - (\theta_1\, v_2/v_1)}$$

DIFFICULTIES.

1. f_ν — REDDENING
2. $B_\nu(T)$ — BLACK BODY FIT MAY NOT BE CORRECT BECAUSE OF UNKNOWN B.C. AND FINITE TEMP. RANGE IN PHOTOSPHERE
3. v — DIFFERENT VELOCITIES FOR DIFFERENT LINES. EXTENDED PHOTOSPHERE → VELOCITY RANGE.

MODELLING NECESSARY.

1987 a IS A GOOD TEST

The temperature comes from the shape of the continuum. But these measurements also include absolute calibration that permits the absolute flux density, f_ν, to be measured to an accuracy of a few percent. Though it is too simple, the assumption of a spherical blackbody allows the combination of temperature, T, and f_ν to yield the angular size :

$$\theta = \frac{R}{D} = \left(\frac{\pi B_\nu(T)}{f_\nu}\right)^{1/2} \quad (1)$$

Of course, we attribute the change in angular size to increasing radius, R, rather than changing distance, D despite substantial secular changes in the extragalactic distance scale. Figure 3 shows that just as you might expect in a violent stellar explosion, the radius of the photosphere increases with time during the first month. Even though the supernova is decreasing in luminosity through the first month after maximum, the decline in temperature is enough to make the inferred radius increase.

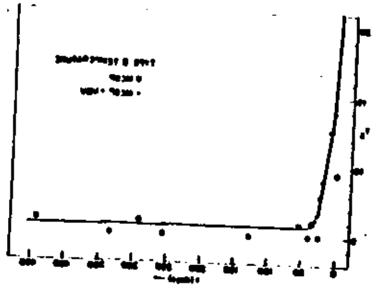

Figure 2. Temperature evolution for a SN II.

Of course, a blackbody is too strong an assumption to use without further investigation, and there are other assumptions involved in the method described here. To help the skeptics keep score, Table 1 lists the principal assumptions, some observations that can be used to check them, and the next step forward in refinement. For the blackbody assumption, comprehensive observations from the UV to infrared are desirable to look for deviations from the Planck law. Model atmospheres, such as those of Kershkovits and Wagoner (1985) are the next step.

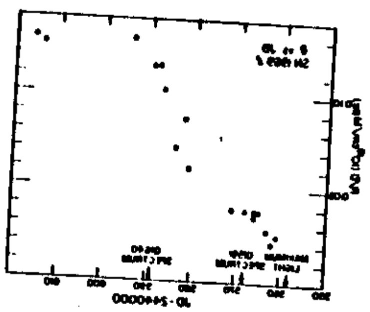

Figure 3. Angular size of the photosphere of a SN II.

On inspecting the photometric scans of supernovae deep in the second sub-basement of Robinson Lab, within earshot of Zwicky himself, Leonard Searle pointed out that the angular expansion can be compared to the rate of expansion inferred from absorption lines to give the distance to the supernova. This was applied by Branch and Patchett (1973) to SN I's and by Kirshner and Kwan (1974) to SN II.

To make some progress, it is necessary to make some assumptions, but they can be checked later against other evidence. If the envelope undergone free expansion after a brief period of acceleration when the emerging shock hits the atmosphere of the star, then material with velocity v will be at a distance R at a time t given by:

$$R = v\,(t - t_0) + R_0 \quad (2)$$

where the initial radius is R_0 at the moment t_0. Now R_0 and t_0 are not accessible to observation so the sensible thing to do is to use two or more observations of the flux, temperature, and velocity separated by a sufficient span of time. Then

$$R(t_1) = v_1(t_1-t_0) + R_0 \quad (3)$$

$$R(t_2) = v_2(t_2-t_0) + R_0 \quad (4)$$

using (3) to eliminate t , we get

$$R(t_2) = v_2(t_2-t_1) + \frac{v_2}{v_1}(R_1-R_0) + R_0 \quad (5)$$

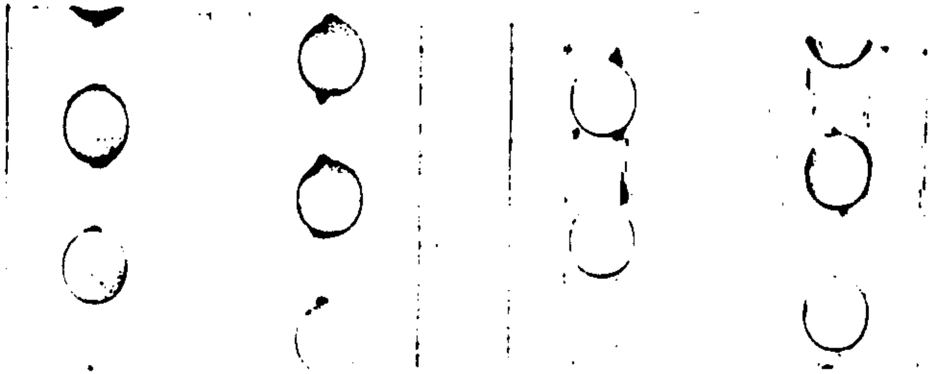

TYPE I AS STANDARD CANDLES

REAL DISPERSION IN TYPE I AT MAXIMUM ?

BRANCH SUGGESTS M_B DEPENDS ON RATE OF DECREASE OF LIGHT CURVE. i.e. THERE IS ANOTHER PARAMETER THAT MUST BE OBSERVED.

RADIO SN

5 TYPE II DETECTED 1950 b, 1957 d, 1970 g, 1979 c, 1980

FAST TURN-ON SLOW DECAY ≳ 1000 DAYS

OPTICALLY THICK AT 20 cm AT FIRST.

1983 ~ (M83) TYPE I b

NON-THERMAL γ = -1.04

POWER LAW DECAY FASTER THAN FOR TYPE II.

MOST PROMISING MODEL (CHEVALIER) INTERACTION REGION BETWEEN EXPANDING SN GAS AND CS ENVELOPE OF SLOW MOVING GAS FROM EARLIER STELLAR WIND.

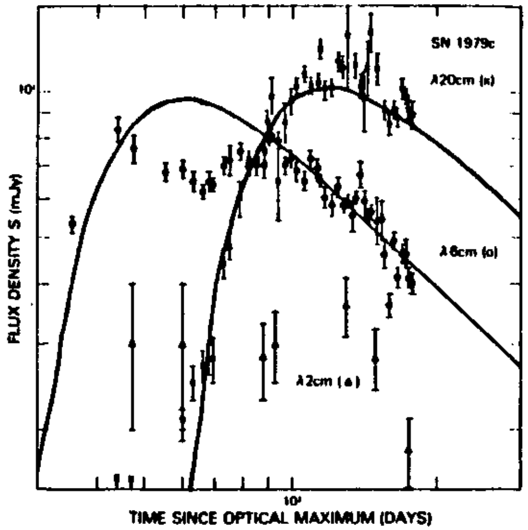

Figure 1: Radio light curves for the Type II supernova SN1979c in NGC4321 (M100). All three wavelengths measured with the VLA are shown together; 20 cm (x), 6 cm (o), and 2 cm (Δ). The "age" of the supernova is measured in days from the date of maximum optical light on 1979 April 19. The solid lines represent the "best" fit of curves of the form $S = K_1 \nu^{\alpha} t^{\beta} e^{-\tau}$ where $\tau = K_2 \nu^{-2.1} t^{\delta}$ with $K_1 = 1.07 \times 10^{6}$, $\alpha = -0.56$, $\beta = -0.92$, $K_2 = 4.31 \times 10^{10}$, and $\delta = -3.54$.

In addition to the detailed studies of SN1979c, we had the good fortune to have a second Type II supernova, also of the subclass "L," appear in the galaxy NGC6946 in 1980 November. Again our radio monitoring was started while the object was still optically bright and this time a year long wait for 6 cm radio emission was not necessary. At an age after maximum optical light of only 35 days, a radio source was detected at 6 cm wavelength at the position of the supernova.

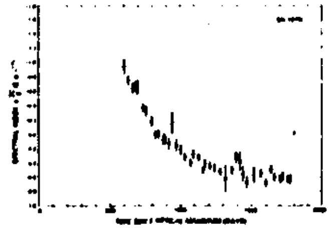

Figure 2. Spectral index (α) for SN1979c between 20 cm and 6 cm ($S \propto \nu^{\alpha}$) plotted as a function of time in days since maximum optical light on 1979 April 19.

In much the same fashion as for SN1979c regular, approximately monthly monitoring of the supernova at both 6 and 20 cm, with less frequent observation at 2 cm, was initiated with the VLA. Detailed light curves have been established for SN1980k and these are shown in Figure 3.

The spectral index change with time for SN1980k is shown in Figure 4 in a manner similar to that for SN1979c in Figure 2.

In summary, we know that at least SN1979c has low linear polarization, being less than 1% polarized at 6 cm wavelength, that both supernovae have fast turn-on times at each wavelength followed by slow declines with time, that they are optically thin first at shorter wavelengths and later at longer wavelengths, and that they are nonthermal emitters having both high brightness temperatures and nonthermal spectral indices.

III. MODELS

In order to try to understand the extensive data sets available for these two Type II supernovae and to relate them to the question of this conference, supernovae as distance indicators, it is necessary to consider the models for their radio emission. Several have been proposed. The simplest and oldest is that of an expanding relativistic gas cloud created essentially instantaneously by an explosion. This balloon of relativistic particles and magnetic fields then expands freely and adiabatically. This model was not developed for supernovae, but for

IR DATA OBSERVED IN [illegible]

PROBABLY TYPE I. GRAHAM ET AL. (1983).

X-RAYS

1980 k NGC 6946 THE ONLY ONE DETECTED.

SUPERWIND AROUND 1984 e (N3169)

NARROW BALMER LINES AT MAXIMUM DISAPPEARED 1 MONTH LATER

SHELL FORMED JUST BEFORE EXPLOSION.

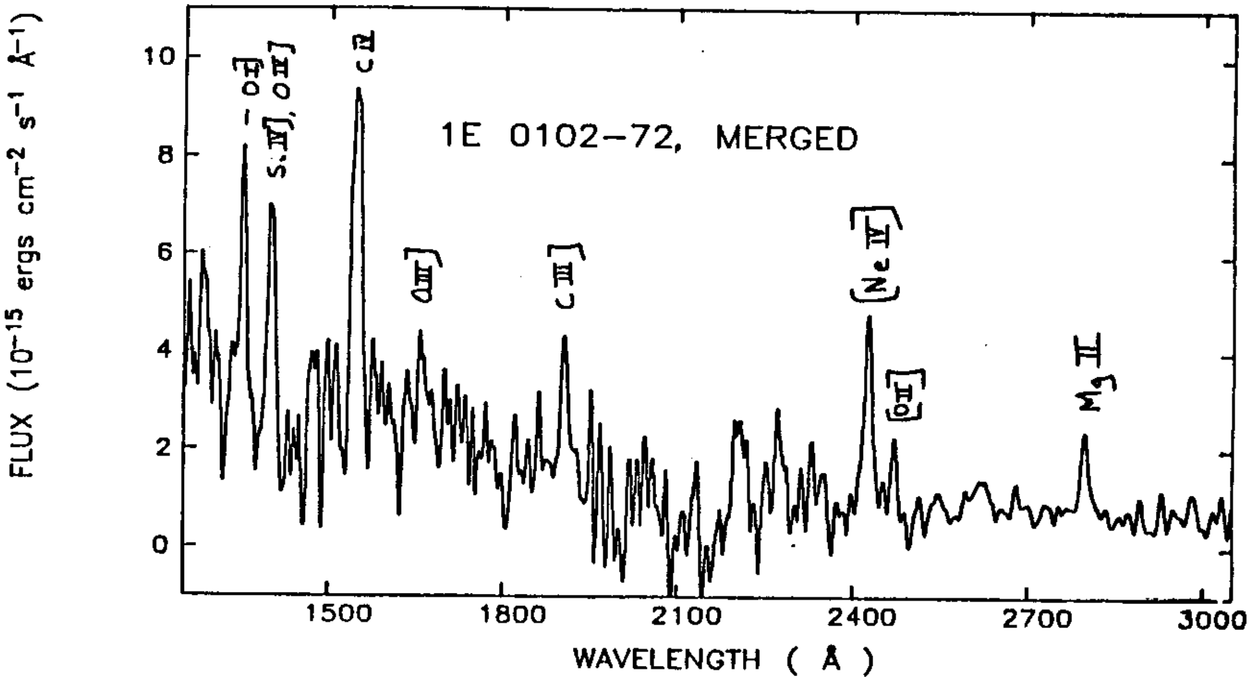
1E 0102-72, MERGED
FLUX (10^-15 ergs cm^-2 s^-1 Å^-1)
WAVELENGTH (Å)
0
2
4
6
8
10
1500
1800
2100
2400
2700
3000
C IV
C III]
[Ne IV]
Mg II

FIGURE 5

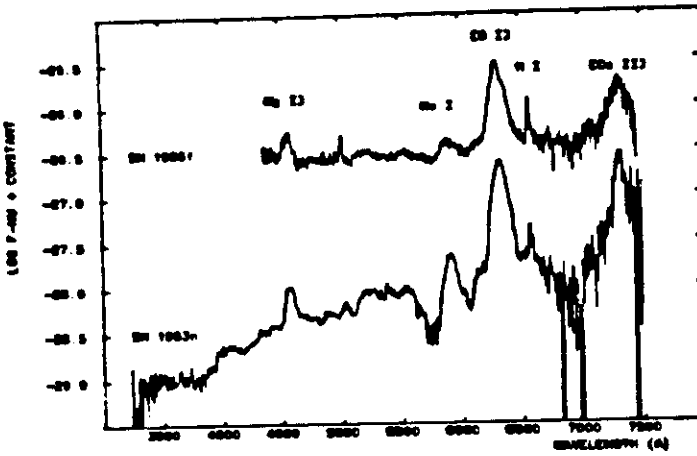

FIG. 1.—The spectrum of SN 1985f in NGC 4618 (top) obtained on 1985 March 25, 25 days after discovery is shown in comparison with a composite spectrum from the nights of February 28, 1984 March 1 of SN 1983n in M83 (NGC 5236) ... host ... class...

ARTICLES

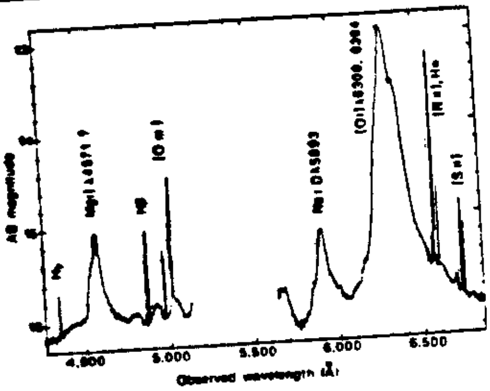

Fig. 1 CCD spectra of the starlike object and its surrounding H II region near the nucleus of NGC4618. Ordinate units are given by AB = −2.5 log (f_ν) − 48.6, where f_ν is in erg s^{-1} cm^{-2} Hz^{-1}, but the blue spectrum is probably ~0.1 mag fainter than displayed here. All narrow lines are associated with the H II region, while the broad features, which strongly resemble those in quasars, are almost certainly produced by a supernova in NGC4618. The data have been smoothed with a gaussian (3 Å FWHM), making the peak intensities of narrow lines appear smaller than in the original spectra.

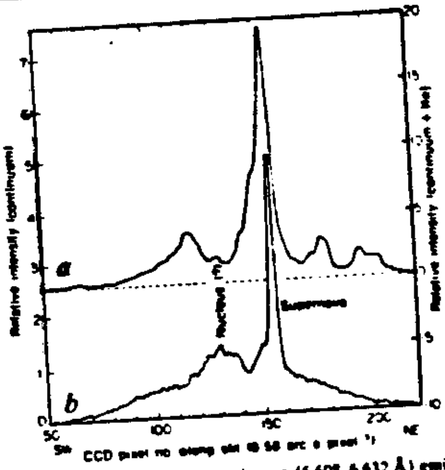

Fig. 2 Plots of the average continuum (6,608–6,632 Å) emission (b) and average continuum plus Hα (6,570–6,578 Å) emission (a) along the central bar in NGC4618. The apparent nucleus, as defined by the continuum, is ~14 arc s from the supernova, although the actual nucleus may be hidden by a thick dust lane near pixel 142 ... Many H II regions are visible, in (a), the most intense of which surrounds the supernova and is brightest on the south-west side.

Hale 5.08-m telescope at Palomar Observatory. The slit (~2 arc min in length) was placed along the conspicuous central bar and included the stellar object. A dichroic filter directly behind the slit reflected blue light (λ ≤ 5,500 Å) to one camera and transmitted red light (λ ≥ 5,500 Å) to the other. Detectors consisted of two charge-coupled devices (CCDs) (Texas Instruments), each with 800 × 800 square pixels. Gratings having 1,200 and 600 grooves mm^{-1} were used in the first order to achieve resolutions (full width at half-maximum, FWHM) of ~2.6 Å and ~4.3 Å in the red and blue cameras (respectively) with a slit width of 2 arc s. The first integration (20 min) covered the intervals λλ4,250–5,125 and λλ6,200–6,850, whereas the second (15 min) provided useful data over λλ3,680–4,120 and λλ5,620–6,280. The seeing was 1.5–2 arc s at all times.

Normal procedures were used to calibrate the spectra. A bias level was subtracted from each data frame, and division by the featureless spectrum of a hot tungsten lamp removed local variations in the sensitivity of the CCDs. Pixels affected by cosmic rays were eliminated by inspection. Wavelengths were determined by fitting cubic polynomials to unblended emission ...

Inspection of the long-slit CCD spectra reveals a series ... H II regions which are presumably responsible for the mott... appearance of the central bar in NGC4618 (Fig. 2). The bright... of these is almost coincident with the starlike object; its p... is displaced by at most ~1 arc s, while its centroid is a few ... seconds away. In the top portion of Fig. 2 it appears a ... 'shoulder' predominantly on one side (south-west) of the un... solved spike. Because the effective entrance aperture for ... spectrum in Fig. 1 is 2 × 8.7 arc s, much of the light from ... H II region is included and it obviously accounts for all ... narrow emission lines. Their relative intensities do not d... substantially from those in other ionized clouds along the ... The ratio I([S II] λ6,716)/I([S II] λ6,731) ≈ 1.40, indicat... that the electron density (n_e) is ≤ 60 cm^{-3}. Assuming nor... Case B recombination[6], a visual extinction of ~1.0 ma... implied by the observed strengths of Hβ and Hγ. This ma... may not apply to the stellar object, depending on its ac... spatial location with respect to the H II region. The narrow ... at ~3,734 Å mentioned earlier is clearly [O II] λ3,727.

Intensities, equivalent widths, wavelengths, and profile wi... (FWHM; full width at zero-intensity, FWZI) of the emis...

-28-

Oke & Searle Ann. Rev. A.A. 1974
Kirshner et al. Ap.J. 185, 303, 1973.
Patchett & Branch MN 158, 375, 1972
Kirshner & Kwan Ap.J. 193, 27, 1974
Panagia et al. MN 192, 861, 1980
Branch et al. Ap.J. 244, 780, 1981.
Kirshner & Oke Ap.J 200, 574, 1975.
Meyerott Ap.J. 239, 257, 1980.
Graham et al. Nature 304, 709, 1983
Branch Ap.J. 258, 35, 1982
Graham et al. MN 218, 93, 1986
Branch et al. Ap.J. 270, 123, 1983
Arnett, Wagoner, Branch, Axelrod Nato 1981 Cambridge ed. Rees et al.
Lecture Notes in Physics 224. Chevalier, Kirshner, Panagia, Wheeler, McCall, Sramek, Weiler, Fransson.